Atmospheric Environment 44 (2010) 533–540

Contents lists available at ScienceDirect

Atmospheric Environment

journal homepage: www.elsevier.com/locate/atmosenv

Ultrafine particles at three different sampling locations in Taiwan

Sheng-Chieh Chen [a], Chuen-Jinn Tsai [a,*], Charles C.-K. Chou [b], Gwo-Dong Roam [c], Sen-Sung Cheng [d], Ya-Nan Wang [d]

[a] Institute of Environmental Engineering, National Chiao Tung University, No. 1001, University Road, Hsinchu 300, Taiwan
[b] Research Center for Environmental Changes, Academia Sinica, No. 128, Academia Road, Section 2, Taipei 115, Taiwan
[c] Office of Sustainable Development, Environmental Protection Administration, No. 83, Sec. 1, Jhonghua Road, Taipei 100, Taiwan
[d] School of Forestry and Resource Conservation, National Taiwan University, No. 1, Section 4, Roosevelt Road, Taipei 106, Taiwan

ARTICLE INFO

Article history:
Received 29 July 2009
Received in revised form
19 October 2009
Accepted 29 October 2009

Keywords:
Atmospheric aerosol
Ultrafine particle
Artifact of organic carbon
Chemical mass closure
Particle effective density

ABSTRACT

Atmospheric ultrafine particles (UPs or $PM_{0.1}$) were investigated at the roadside of Syuefu road in Hsinchu city, in the Syueshan highway tunnel in Taipei and in the NTU Experimental Forest in Nantou, Taiwan. A SMPS (TSI 3936) and three MOUDIs (MSP 110) were collocated to determine the number and mass concentrations of the $PM_{0.1}$ simultaneously. The filter samples were further analyzed for organic carbon (OC), element carbon (EC), water-soluble ions and trace elements. Taking into account the OC artifact of $PM_{0.1}$, good chemical mass closure (ratio of the reconstructed chemical mass to the gravimetrical mass of PMs) was obtained with an unknown percentage of 10.6, 26.2 and 37.2% at the roadside, tunnel and forest, respectively. The unexplained mass was attributed to aerosol water in this study. The artifact at the roadside, tunnel and the forest $PM_{0.1}$ mass was found to be as high as 51.6 ± 10.7%, 20.0 ± 5.4% and 85.6 ± 18.4%, respectively. Finally, the effective density of the roadside, tunnel and forest $PM_{0.1}$ was calculated based on the results of chemical speciation and found to be 1.45, 1.29 and 1.22 g cm^{-3}, respectively, which was in good agreement with that obtained by using the method of Spencer et al. (2007). Based on these results, it is foreseeable that the number concentration of the SMPS can be converted using the effective density determined by Spencer et al. (2007) for the real time measurement of the $PM_{0.1}$ concentration.

1. Introduction

Researchers have found associations between the adverse health effects and the exposure of ultrafine particles (UPs or $PM_{0.1}$) (Donaldson et al., 2002; Oberdörster et al., 2005) which also could influence the visibility, global climate and participate the atmospheric chemistry (Seinfeld and Pandis, 1998). These adverse effects of UPs could be attributed to their small size, high number concentration as well as bounded elemental/organic carbon, sulfate, elements and PAH (polycyclic aromatic hydrocarbons) on them. Therefore, it is very important to measure the mass and chemical species concentrations of $PM_{0.1}$ accurately to assess these effects.

The particle density is an important physical property of particles, which can be calculated according to chemical composition of particles (McMurry et al., 2002). However, it is often difficult to obtain the composition of particles accurately, especially UPs, due to its chemical complexity and the formation of OC artifact which leads to error on determining the concentration of POC (particulate organic carbon). The OC artifact is resulted from the adsorption of gaseous OC or the volatilization from the collected particles on the filter (Chen et al., submitted for publication; Turpin et al., 2000). In our previous study (Chen et al., submitted for publication), the artifact was corrected adequately by using the QBQ (Quartz Behind Quartz) and QBT (Quartz Behind Teflon) methods proposed by Subramanian et al. (2004) and good chemical mass closure (ratio of the reconstructed chemical mass to the gravimetrical mass) for $PM_{0.1}$ was obtained.

The density can be used to determine the relationship between the Stokes and aerodynamic diameters and is obtained by taking the ratio of the gravimetric mass to the measured volume (calculated from size distribution). Stein et al. (1994) used the DMA (differential mobility analyzer)-impactor technique developed by Kelly and McMurry (1992) to measure the density of 0.1–0.25 μm atmospheric particles in Meadview, AZ. They found that the density ranged from 1.60 to 1.79 g cm^{-3} and tended to decrease with increasing relative humidity. It is important to note that the combined measurement of mobility (SMPS, Model 3936, TSI Inc., MN, USA) and aerodynamic diameters (impactor, MOUDI, Model 110, MSP Corp., MN, USA) yields particle density only if the particles are spherical. However, most of the atmospheric particles are

* Corresponding author. Tel.: +886 3 573 1880; fax: +886 3 572 7835.
E-mail address: cjtsai@mail.nctu.edu.tw (C.-J. Tsai).

1352-2310/$ – see front matter © 2009 Elsevier Ltd. All rights reserved.
doi:10.1016/j.atmosenv.2009.10.044

nonspherical (De Carlo et al., 2004) and the effective density is often used instead (Kelly and McMurry, 1992).

Khlystov et al. (2004) and Shen et al. (2002) compared the mass concentrations of PM determined by the MOUDI and the SMPS–APS. The particle effective density of 1.5–1.6 g cm^{-3} was assumed in the studies. Both of them found the SMPS underestimated $PM_{0.1}$ mass significantly compared to the MOUDI. It was because that particle bounce occurred at the stages of the MOUDI as it was observed that the SMPS–APS overestimated particle mass in the accumulation mode compared to the MOUDI. Park et al. (2003) used the DMA–APM (particle mass analyzer) technique to determine the effective density of diesel particles and then converted the number distribution of the SMPS to mass distribution. The converted mass distribution was compared with that of the MOUDI. They found the effective density of diesel particles decreased with increasing particle sizes, which was around 1.0, 0.8, 0.6 and 0.5 g cm^{-3} for particles of 50, 100, 150 and 300 nm in mobility diameter. Although more accurate effective density of particles was obtained by Park et al. (2003), they also found the MOUDI oversampled UPs for sizes below 60 nm due to particle bounce. Therefore, it is important for this study to reduce particle bounce first by coating the substrates of the MOUDI carefully and then conduct the conversion of the mobility to aerodynamic diameter so that the $PM_{0.1}$ concentrations determined from the MOUDI and SMPS can be compared.

Spencer et al. (2007) used the DMA–ATOFMS (aerosol time-of-flight mass spectrometer, Model 3800, TSI Inc., MN, USA) to study the effective density of ambient aerosols. In order to study if there were chemical/physical changes leading to the change in the effective density over the different sampling periods, the author compared the average effective density with the ambient ozone concentration, relative humidity and absolute atmospheric water content. They found the particle density was influenced mostly by the atmospheric water content. In Park et al. (2003) and Spencer et al. (2007), the effective density was studied for classified monodisperse urban or diesel nanoparticles only. But up to now, the average effective density has not been studied for $PM_{0.1}$ at different sampling locations.

Hänel (1976) pointed out liquid water constitutes a significant mass fraction of the aerosol mass of total PM even at relatively low RH of 30%. Tsai and Kuo (2005) found water contributed 22–27% to the mass of urban $PM_{2.5}$ in a southern city of Taiwan when the average RH and temperature were 60% and 25.0 °C, respectively. Aggarwal and Kawamura (2009) found the ambient submicron particles (15–750 nm) in Sapporo, Japan, contained about 30% mass of particles at the RH of 71% and the temperature of 23.6 °C. From these studies, it can be said that water constitutes a significant amount of mass of different PM fractions.

Ambient particles are multi-components which consist of primary and secondary organics, inorganic salts (such as sulfate, nitrate, chloride and sodium), inorganic carbon and elements, as well as water. Pilinis et al. (1989) pointed out that the ambient aerosols exhibit similar behavior to single component salts, including the deliquescence and hysteresis processes. They predicted that the deliquescence RH of urban aerosols was about 60%, which is the same as that calculated by Nenes et al. (1998). Pilinis et al. (1989) further found when the RH reduced from a RH higher than the deliquescence RH of 85–35% at 25 °C, the aerosol water content of the urban aerosols was reduced from 65% to 25%. Deliquescence RH was also found to decrease with increasing temperature for both single salt and mixed salts (Tang and Munkelwitz, 1993; Seinfeld and Pandis, 1998).

For organic aerosols (containing organic acids), Demou et al. (2003) found that most organic compounds bounded on the aerosols were water-soluble substances. The growth of organic aerosols is primarily due to the condensation of trace organics onto the existing particles. As pointed out by Ellison et al. (1999), atmospheric particles whose surface is composed of organic molecules are subject to surface oxidation by OH, O_3, NO_3 and halide species. The particles that are initially hydrophobic will gradually become more hydrophilic due to surface oxidation, and then act as the condensation sites for water and trace organic species. Demou et al. (2003) found that the particles composed of organic acids showed a similar deliquescence and hysteresis processes to those observed for multi-component inorganic salts. Very little water was given off as the RH was decreased from 100% until a sudden water loss occurred at 35% RH.

Most of the previous studies focused on the particle density and water content for total PM and $PM_{2.5}$ only. In this study, $PM_{0.1}$ at different atmospheres including a roadside, a highway tunnel and a forest was investigated. The MOUDI was used to collect $PM_{0.1}$ and the SMPS was used to measure its number concentration. In addition to the gravimetric analysis of the MOUDI filter samples, chemical compositions including organic carbon (OC), element carbon (EC), 9 water-soluble ions and 19 trace elements were also obtained. The chemical mass closure for $PM_{0.1}$ was obtained first by taking into account the correction of the OC artifact. Based on the concentrations of the chemical components, the effective density of $PM_{0.1}$ was calculated assuming the unknown chemical mass was water. The calculated effective density was then compared with that obtained by using the method of Spencer et al. (2007) to assess its accuracy. If the effective density determined by Spencer et al. (2007) is accurate, then the number concentration data of the SMPS can be converted to the $PM_{0.1}$ mass concentrations in real time.

2. Experimental methods

2.1. Site descriptions

Field samples were collected at the height of 1.5 m at the roadside of Syuefu road in Hsinchu, a relay station inside the Syueshan highway tunnel in Yilan and in the NTU (National Taiwan University) Experimental Forest in Nantou, Taiwan. Syuefu road has two directions with only one lane of 4 m in width in each way. There are six schools within a distance of 800 m and it is one of the main roads entering the Hsinchu Science Park. Thus, there is heavy traffic flow during the morning and evening rush hours when commuters as well as the neighborhood residents may exposure to high concentration of PMs. Sampling was conducted at the sideway at one side and at the midpoint of the 800 m-long road, at a distance of about 4 m from the edge of the traffic lane.

The Syueshan highway tunnel is the longest road tunnel in Taiwan with a total length of 12.9 km. Only shuttle buses, passenger cars and light-duty diesel trucks are allowed in the tunnel. The tunnel has two two-lane bores and inclines downward from the west (Pinglin direction, Taipei County) to the east (Toucheng direction, Yilan County) with a slope of 1.3%. There are three ventilation and three relay stations located alternatively with equal distance of about 2 km in between stations. These stations are located at 1.5, 3.5, 5.5, 7.5, 9.5, 11.5 km from the entrance of tunnel. Sampling was conducted at one of the three relay stations located 1.4 km from the outlet (Toucheng, 11.5 km from the inlet Pinglin). The tunnel does not have distinct morning and evening rush hours, which only occurs during the weekend and holidays. In each ventilation station, a huge fan was installed in one vertical well to transport outer cleaner air into the tunnel and while the other fan was installed in another well to exhaust polluted air outside of the tunnel. However, these fans are seldom activated because the total amount of traffic flow in the tunnel is restricted. The fans in the relay stations, which exchange the air between the two bores are

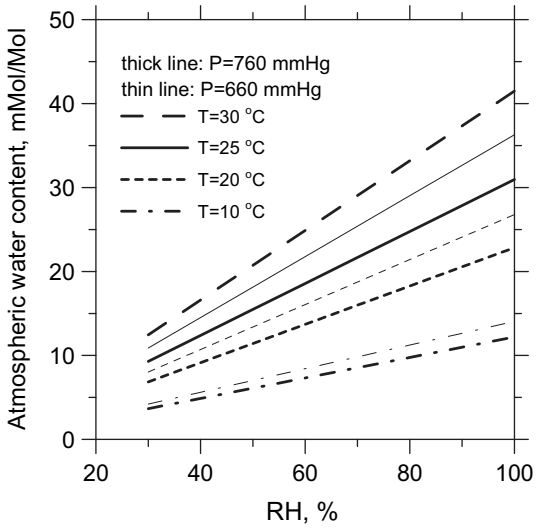

Fig. 1. Relationship between the absolute atmospheric water content and RH at different temperatures and atmospheric pressures.

also normally closed. There are two axial fans mounted on the top of the bores at every 0.5 km along the tunnel. They are activated when the temperature reaches 40 °C.

The NTU Experimental Forest is located in central Taiwan and belongs to Lugu, Shueili and Sinyi townships in Nantou County. The forest rises from 220 m above the sea level at the southern bank of Jhuoshuei River to 3952 m above the sea level at the peak of Yushan, covering 327.8 km^2 and occupying about 1% of Taiwan Island. The sampling site was located near the center of the forest with an altitude of 1500 m. The Cryptomeria, a genus of conifer, is the most abundant trees surrounding the site.

Sampling was conducted from January to December of 2008, during which six 24-h samples were taken at the roadside, ten 3-h samples were taken in the tunnel at daytime (during AM 09:00–PM 09:00) and six 96-h samples were taken in the forest.

2.2. Sampling protocol

In this study, $PM_{0.1}$ samples were collected at the after filters of the three 10-stage MOUDIs (Model 110, MSP Corp., MN, USA) operated in parallel. The nozzle plates of the 10th stages were removed so that the after filters sampled only $PM_{0.1}$ particles. A collocated SMPS (Model 3936, TSI Inc., MN, USA) equipped with Nano-DMA (TSI Model 3085) and Ultrafine Water-based Condensation Particle Counter (UWCPC, TSI Model 3786) was used to monitor the number concentrations of ambient particles from 5 to 200 nm simultaneously. A detailed description of sampling procedure is described in our previous paper (Chen et al., submitted for publication). Briefly, in two MOUDIs (M1 and M2), silicone grease coated aluminum foils were used as the impaction substrates in 0–9 stages to reduce solid particle bounce (Pak et al., 1992). Teflon (Zefluor P5PJ047, Pall Corp., New York, USA) and quartz filters (Tissuquartz 2500QAT-UP, 7201&7202, Pall Corp., New York, USA) were used in M1 and M2, respectively, as the after filters to collect $PM_{0.1}$ for further gravimetric (M1 only) and chemical analysis (both M1 and M2). The third MOUDI (M3) was used to determine the positive artifact of OC, in which a HEPA filter (HEPA Capsule 12144, Pall Corp., New York, USA) was installed at its inlet to remove all particles. In M3, the impaction substrates from stage 0–9 were not used while only two quartz filters (QBH, quartz behind HEPA; QBH1, quartz behind QBH) were placed at the after filter stage. Thus, both the gaseous OC and the volatilized OC from the particles collected on the HEPA was adsorbed on the two quartz filters. The $PM_{0.1}$ concentration of MOUDI (M1) was compared with the calculated $PM_{0.1}$ concentration based on the SMPS data and apparent particle density determined using the method of Spencer et al. (2007).

In addition to sampling $PM_{0.1}$, the concentrations of gaseous pollutants CO and SO_2 were measured at roadside and tunnel sites. The concentrations of CO were measured continuously by using a CO Analyzer (Model 48*i*-TLE, Thermo Environmental Inc., USA). Concentrations of SO_2 were measured by a SO_2 Analyzer (Model 43A, Thermo Environmental Inc., USA). Moreover, meteorological parameters, including temperature, relative humidity, wind direction and wind speed were recorded at all three sites. A video camera was used to record the traffic flow and compositions at both traffic sites.

2.3. Sample analysis

A detailed description of the sample analysis can be found elsewhere (Chen et al., submitted for publication) and is described briefly in the following. Before chemical analysis, Teflon sample of M1 was weighed first to determine the mass concentrations of the $PM_{0.1}$. The electrostatic charge of the filters was eliminated by a constant ionizing air blower (Model CSD-0911, MEISEI, Japan) before weighing. A microbalance (Model CP2P-F, Sartorius, Germany) was used after the filters were conditioned at least 24-h in a temperature and relative humidity controlled room (23 ± 1 °C, 40 ± 5% RH). After gravimetric analysis, the Teflon filter was cut equally in half using a Teflon coated scissors. One half was analyzed by ICP-MS (Model 7500 series, Agilent Technologies, Inc., USA) for elements except Si which was analyzed by ICP-AES (Model Optima 2000DV for Si, PerkinElmer, Inc., MA, USA) and the other half was analyzed by ion chromatograph (IC, Model DX-120, Dionex Corp, Sunnyvale, CA) for ionic species. The analyzed elements included crustal elements (Na, Mg, Al, K, Ca, Fe and Si) and anthropogenic elements (S, Zn, Ni, Cu, Mn, Sr, Ag, Ba, Pb, V, Cr and Ti). The analyzed ions were F^-, Cl^-, NO_3^-, SO_4^{2-}, NH_4^+, Na^+, K^+, Mg^{2+} and Ca^{2+}.

The quartz filter samples of the M2 and M3 were analyzed by thermal-optical reflectance (TOR) method for OC and EC concentrations without gravimetric analysis. The method in Chen et al. (submitted for publication) was used to determine the POC concentration. POM (particulate organic mass) was then estimated by multiplying 1.4, 1.6 and 2.1 to the POC at the tunnel, roadside and forest, respectively (Geller et al., 2005; Turpin and Lim, 2001).

Adding the concentrations of POM, EC, elements and soluble ions for $PM_{0.1}$, the chemical reconstructed mass concentrations was compared with the gravimetric mass concentration. To compare the mass concentration calculated from the number distributions of the SMPS with that obtained from the M1, the particle mobility diameter of the SMPS was converted to the aerodynamic diameter using an effective density, ρ_{eff}, which was related to the absolute atmospheric water content, mMol Mol^{-1}, obtained by Spencer et al. (2007). The absolute atmospheric water content, $[H_2O]$, was calculated as (Seinfeld and Pandis, 1998):

$$[H_2O] = 10 \times RH \frac{p^0_{H_2O}}{p}, \quad (\text{mMol Mol}^{-1}) \tag{1}$$

where p is the atmospheric pressure (Pa); RH is the relative humidity (%); and $p^0_{H_2O}$ is the saturation vapor pressure (Pa) which can be calculated as (McRae, 1980):

$$p^0_{H_2O}(T) = p_s \exp\left[13.3185a - 1.9760a^2 - 0.6445a^3 - 0.1299a^4\right] \tag{2}$$

where p_s is the standard atmospheric pressure of 101.3 kPa, and the parameter a is defined in terms of the ambient T(K) and the steam temperature T_s (373.15 K) at p_s as $a = 1 - T_s/T$. According to Eqs. (1) and (2), the relationship between the absolute atmospheric water content and RH at different temperatures and pressures ($P = 760$ mmHg at the roadside and tunnel; $P = 660$ mmHg at the forest) was calculated and the result is shown in Fig. 1. It is seen the water content increases with increasing RH at a fixed temperature and pressure while it also increases with increasing temperature and decreasing pressure at a fixed RH. According to Fig. 4 of Spencer et al. (2007), the effective density of particles, Y, can be calculated based on the absolute atmospheric water content, X, as:

$$Y = -0.0012X^2 + 0.0076X + 1.5114, \quad 0 < X \leq 24 \tag{3}$$

It is to be noted that Eq. (3) was based on urban particles of several hundred nanometers (Spencer et al., 2007). It was used in this study to calculate the effective density of $PM_{0.1}$ and compared with that determined by chemical compositions. Besides, Y was assumed to be equal to 1.0 as $X > 24$ (very high absolute atmospheric water content) in this study.

When the effective density was obtained, the mobility and aerodynamic diameters conversion was made using the following equation (Sioutas et al., 1999; Khlystov et al., 2004):

$$d_m = \frac{d_a}{X}\sqrt{\frac{C(d_a)}{C(d_m)}}, \quad X = \sqrt{\frac{\rho_p}{\kappa\rho_0}} = \sqrt{\frac{\rho_{eff}}{\rho_0}} \tag{4}$$

where d_m is the mobility equivalent diameter, d_a is aerodynamic diameter, $C(d_a)$ is the slip correction factor corresponding to d_a, $C(d_m)$ is the slip correction factor corresponding to d_m, X is the size-correction factor, κ is the dynamic shape factor, ρ_p is the density of the particle, and ρ_0 is the unit density (1 g cm^{-3}). By using Eq. (4), the $PM_{0.1}$ mass concentration was then calculated from the SMPS data by summing the converted mass concentrations of all size intervals below 100 nm in aerodynamic diameter. For each size interval, the number concentration of SMPS was converted to mass concentration using the following equation:

$$C_m = \frac{\pi}{6}\rho_{eff}N_c d_m^3 \tag{5}$$

where, C_m is the mass concentration and N_c is the number concentration.

3. Results and discussion

3.1. Size distribution of UPs

Fig. 2 shows a typical variation of total $PM_{0.1}$ number concentration and size distribution with the traffic flow rate, SO_2 and CO concentrations of the Syuefu roadside on Sep. 9–10, 2008. This pattern is identical for all roadside measurements so that the results of the others are not presented. As can be seen from the figure, the total number concentration of $PM_{0.1}$ and the size distribution are strongly related to the traffic flow rate, SO_2 and CO concentrations, revealing that the emission of UPs is representative of local motor emissions. It is to be noted, the traffic flow rate shown in Figs. 2 and 3 were obtained by counting total number of vehicles passing through the site, which were dominated by nearly equal number of motorcycles and passenger cars. In the morning rush hour (08:00–10:00), a high $PM_{0.1}$ number concentration of 1.3×10^5 # cm^{-3} with the mode size of 10–30 nm was observed, which was due to a very close proximity between the vehicle emission and the sampling location (within 4 m). That is, the SMPS would sample fresh nanoparticles emitted from the vehicles. During the sampling period, the wind speed was measured to be low, typically less than 3 km h^{-1}. The mode particle size of 10–30 nm at the roadside was almost the same as that measured at the roadside of 710 freeway in CA by Zhu et al. (2002) who found particles at the roadside existed in two modes at 10 and 20 nm, respectively. One hour later to the early afternoon (11:00–14:00), particle concentration of $PM_{0.1}$ showed a high value of about 1.1×10^5 # cm^{-3} due to photochemical reaction even though the traffic rate was much lower than the morning rush hour. At about 14:30, the sudden occurrence of cloudy weather led to a dramatic reduction of particle number concentration, which explains the importance of sunlight to the formation of SOA. After 16:00 when the cloud coverage decreased, the number concentration of particles was increased again with the increasing traffic flow. However, in the evening rush hours (17:30–19:00) when the traffic rate was similar to the morning, the total particle number concentration of $PM_{0.1}$ was significantly lower than the morning due to the lack of photochemical reaction. In the midnight, the $PM_{0.1}$ number concentration was reduced to less than 1.0×10^4 # cm^{-3} due to very low contribution of motor emission. From these results, it can be concluded that the motor emission of UP number increased with

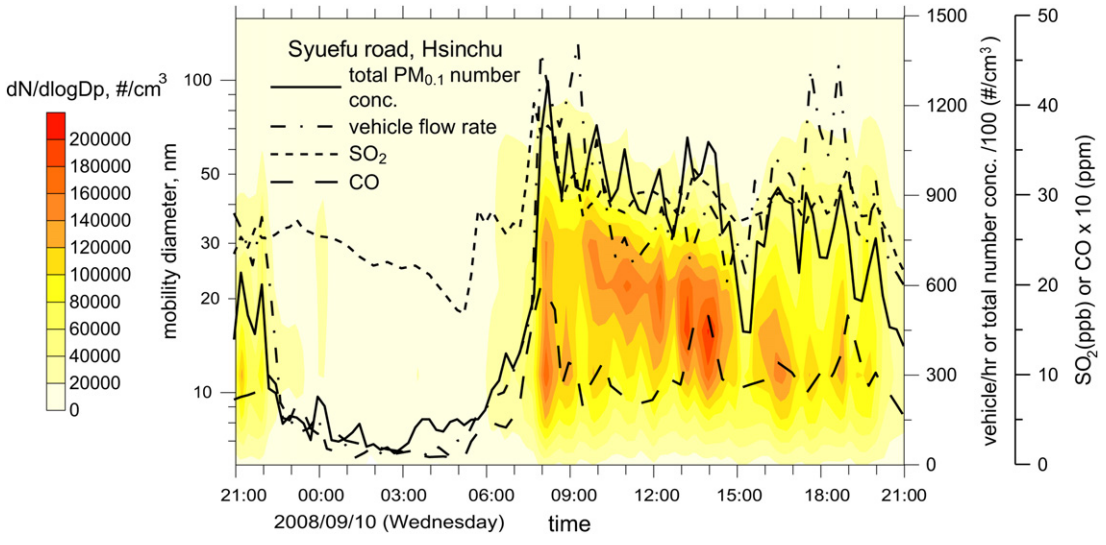

Fig. 2. A typical time variation of particle size distribution and total number concentration of $PM_{0.1}$ at the Syuefu road.

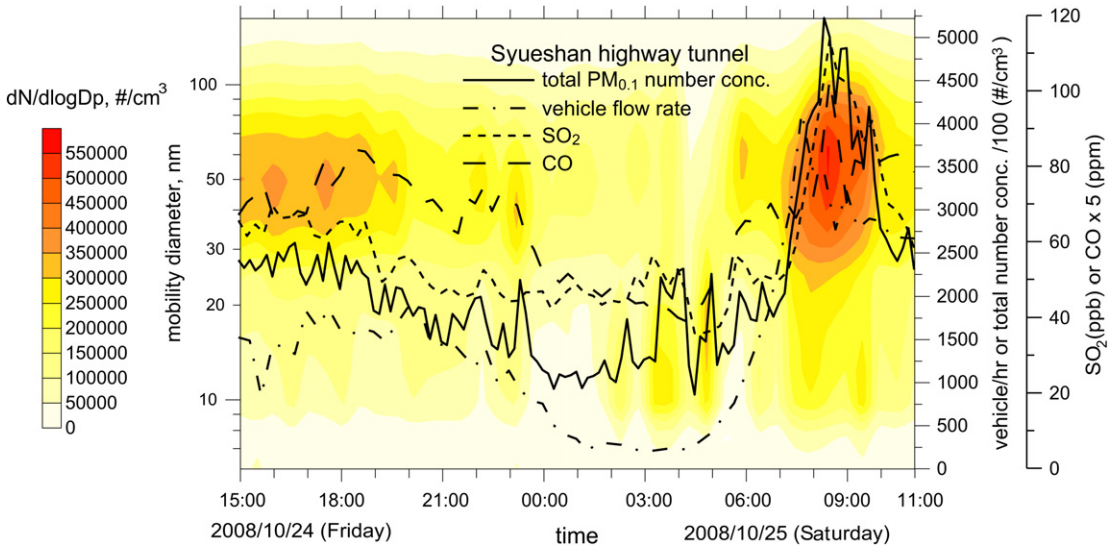

Fig. 3. A typical time variation of particle size distribution and total number concentration of $PM_{0.1}$ in the Syueshan highway tunnel.

increasing traffic flow rate and the sunlight intensity. Similar to the UP concentration, the SO_2 and CO also increased with the increasing traffic flow rate, both peaked at the morning rush hour with the concentrations of 40 ppb and 2 ppm, respectively.

Fig. 3 shows the variation of particle size distribution and total number concentration of $PM_{0.1}$ with the traffic flow rate from a workday afternoon (15:00, Fri., 2008/10/24) to a holiday rush hour (11:00, Sat., 2008/10/25), at the relay station 3. Results of other sampling days are similar and will not be repeated here. The concentration of gaseous pollutants of vehicles, SO_2 and CO, is also shown in the figure. The average composition of vehicles at daytime for the passenger cars, the light-duty diesel trucks and shuttle buses was 91.6 ± 3.6 (average ± one standard deviation), 6.5 ± 2.7 and 1.9 ± 0.4%, respectively. The passenger cars dominated the motor emissions in the tunnel.

It is seen the concentration of $PM_{0.1}$, SO_2 and CO increased with the increasing vehicle flow. A relative high concentration of $PM_{0.1}$ ($\sim 5.25 \times 10^5$ # cm^{-3}) occurred in the Saturday morning rush hour compared to the other periods, when the total number of vehicles and particle size peaked at 4000 vehicles h^{-1} and 50–60 nm, respectively. In other time periods, particles at the 3rd relay station also showed a similar mode diameter. The present mode diameter of 50–60 nm at the 3rd relay station (11.5 km from the entrance) was much larger than 15–20 nm in the Caldecott Tunnel (Geller et al., 2005) because particles had more time to grow via coagulation and vapor condensation in the present long tunnel than in the short Caldecott Tunnel of 1.1 km. The SMPS detected small nanoparticles of size 7–10 nm with a relatively lower concentration ($2.3–3.9 \times 10^4$ # cm^{-3}) due to primary motor emission of nanoparticles, which was similar to those found at the present roadside sampling site and in Caldecott Tunnel. During the rush hour, the concentration of CO and SO_2 was as high as 20 ppm and 110 ppb, respectively, which was much higher than that at the Syuefu road. Comparing the number of vehicles with the number concentration of $PM_{0.1}$, it is found the peak number concentration of $PM_{0.1}$ lags behind the peak traffic flow by about half an hour. On the other hand, the peak number concentration of $PM_{0.1}$ and the peak traffic occurred nearly simultaneously at the roadside. This was because the speed of vehicles (50–70 km h^{-1}) is much higher than the gas flow ($\sim$10 km h^{-1}) which was driven by the piston effect in the tunnel. UPs moved with the gas flow in the tunnel and lagged behind the traffic flow. Comparing the size distributions of the roadside and tunnel sites, the mode diameter of nanoparticles at the rush hour were found to be in sizes 10–30 and 40–70 nm, respectively. The higher total number concentration of $PM_{0.1}$ with larger particle size resulted in a much higher $PM_{0.1}$ mass concentration in the tunnel than that at the roadside.

Similar to Figs. 2–4 shows a typical variation of particle size distribution and total number concentration of $PM_{0.1}$ with RH and temperature during a day (21:00, 2008/12/23–21:00, 2008/12/24) in the NTU Experimental Forest. It is seen the total number concentration of $PM_{0.1}$ generally increases with the decreasing RH and increasing temperature. Similar to the roadside, the total $PM_{0.1}$ number concentration increased to 1.2×10^4 # cm^{-3} at 2:00–3:00 PM due to photochemical reaction when the RH was reduced dramatically and the temperature was peaked at 16 °C. The mode diameter of nanoparticles was in between 30 and 70 nm, which is similar to that of the SOA (Kavouras et al., 1999). From the figure, it is also seen there were primary emitted particles in size 5–10 nm through the day, which were organic acids formed via the photochemical reaction (Kavouras et al., 1998; Kavouras and Stephanou, 2002).

3.2. Chemical mass closure of $PM_{0.1}$

Table 1 shows the comparison of the reconstructed chemical mass concentration (OM + EC + Ion + Element) with the gravimetric mass and the SMPS converted mass concentrations of $PM_{0.1}$ at three different sites. The average mass concentration of each chemical species and the effective $PM_{0.1}$ density at the three sites are also shown in Table 1. According to the temperature and humidity records during the sampling runs, the average effective density of $PM_{0.1}$ was calculated by using Eqs. (1)–(3) to be 1.40 ± 0.10, 1.25 ± 0.14 and 1.15 ± 0.15 g cm^{-3} at the roadside, tunnel and forest, respectively, as shown in Table 1. Using the calculated effective densities of $PM_{0.1}$ at each sampling sites to calculate the converted SMPS mass concentration, good agreement was found between the average $PM_{0.1}$ of MOUDI and SMPS for all three sites.

As shown in Table 1, the MOUDI overestimated $PM_{0.1}$ slightly by about 20–30% compared to the SMPS. The relationship between the $PM_{0.1}$ concentration of the MOUDI and SMPS at the roadside, tunnel and forest is:

$$PM_{0.1,\,MOUDI} = (1.24 \pm 0.28) \times PM_{0.1,\,SMPS} \quad \text{(roadside)} \qquad (6)$$

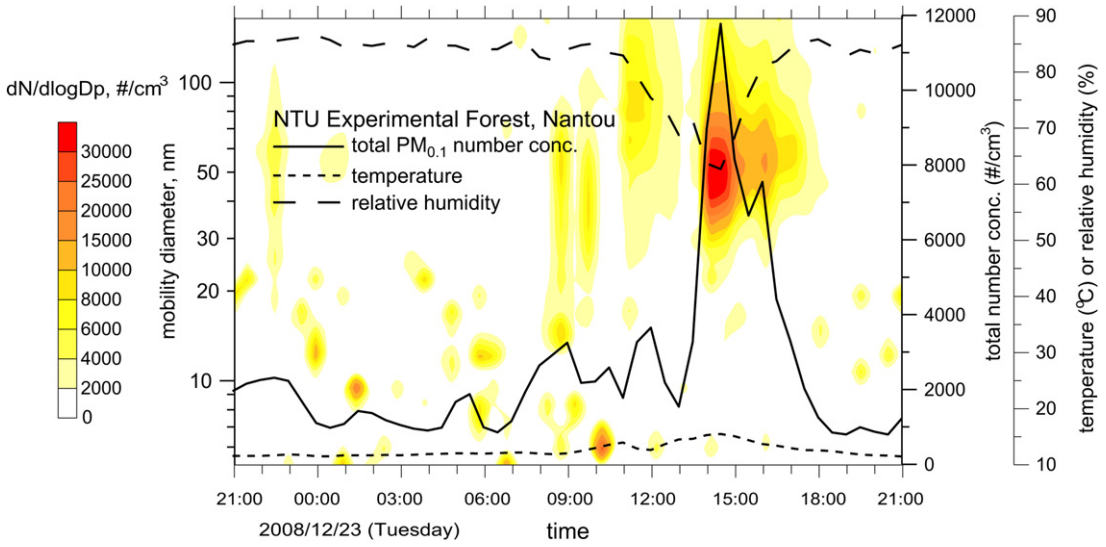

Fig. 4. A typical time variation of particle size distribution and total number concentration of $PM_{0.1}$ in the NTU Experimental Forest.

$$PM_{0.1,\,MOUDI} = (1.18 \pm 0.17) \times PM_{0.1,\,SMPS} \quad \text{(tunnel)} \qquad (7)$$

$$PM_{0.1,\,MOUDI} = (1.33 \pm 0.24) \times PM_{0.1,\,SMPS} \quad \text{(forest)} \qquad (8)$$

The present comparison implies that particle bounce was significantly eliminated in the MOUDI in this study as compared to Khlystov et al. (2004) and Shen et al. (2002). The reduction of bounce in the upper stages of the $PM_{0.1}$ after filter was attributed to the use of coated foils through stages 0–9 in the MOUDI. In comparison, Khlystov et al. (2004) used uncoated substrates, and Shen et al. (2002) only coated the substrate of the 2.5 μm stage in the MOUDI. Because the agreement of $PM_{0.1}$ mass concentration of the MOUDI with that of the SMPS, the species concentrations of $PM_{0.1}$ determined in this study are accurate.

Fig. 5(a)–(c) show the comparison of chemical compositions (%) of $PM_{0.1}$ at the roadside (the mean of all six measurements), in the tunnel (the mean of ten daytime measurements) and in the forest (the mean of all six measurements), respectively. By using the QBQ and QBH methods, the OC artifact was found to account for 51.6 ± 10.7, 20.0 ± 5.4 and 85.6 ± 18.4% of $PM_{0.1}$ mass at the roadside, tunnel and forest, respectively. Severe OC artifact in $PM_{0.1}$ found at the forest and roadside is due to a relative low $PM_{0.1}$ mass concentration and a long sampling time when compared to the tunnel. In the figure, good chemical mass closure is seen at all three sites. The unknown composition was 10.6% at the roadside while a higher unexplained mass was found at the tunnel and forest sites, which was 26.2 and 37.2%, respectively. The achievement of good mass closure for $PM_{0.1}$ of this study indicates the correction of OC artifact is accurate and the use of the POC to POM ratio is adequate.

OM were found to be the most abundant species in $PM_{0.1}$ at all three sites, which agrees with other urban or roadside measurements (Cass et al., 2000; Phuleria et al., 2007; Spencer et al., 2007), the tunnel or chassis dynamometer studies (Geller et al., 2005; Kleeman et al., 2000) and the forest studies (Kavouras et al., 1998, 1999). OM accounted for 38.7 ± 3.3, 31.4 ± 5.1 and 30.4 ± 6.6% $PM_{0.1}$ mass for the roadside, tunnel and forest, respectively. The second abundant species was EC, which was 16.1 ± 7.5, 27.8 ± 5.4 and 13.0 ± 4.6% at the roadside, tunnel and forest, respectively. The mass percentage of ion and element of $PM_{0.1}$ for the roadside, tunnel and forest was 24.8 ± 9.3, 3.0 ± 1.6 and 11.5 ± 4.5%, and 11.3 ± 3.3, 11.6 ± 2.6 and 7.9 ± 2.3%, respectively.

3.3. Effective density of $PM_{0.1}$ at different locations

As mentioned previously, the unexplained mass of $PM_{0.1}$ is 10.6, 26.2 and 37.2% at the roadside, tunnel and forest, respectively. According to the finding of Nenes et al. (1998) and Pilinis et al. (1989), atmospheric aerosols in the urban area have a deliquescence RH of about 60% due to their multi-component constituents of inorganic salts and organic acids (Pilinis et al., 1989; Demou et al., 2003). The average RH during each sampling period at both forest and roadside locations was greater than 65% RH, or greater than the deliquescence RH of $PM_{0.1}$. In addition, Pilinis et al. (1989) and Demou et al. (2003) found that aerosol water would not give off significantly until a relative low RH of 35% was reached. The records of RH at the forest and roadside sites showed the lowest RH was all greater than 40%. Besides, the filter samples were conditioned at 38–43% RH and 22 °C in this study. Therefore, it is reasonable to assume that the unexplained mass of the forest and roadside $PM_{0.1}$ was attributed mostly to aerosol water.

For the present vehicle emission dominated tunnel, it was found that there was 31.4% of $PM_{0.1}$ mass contributed from OM. Fraser et al. (1998) and Schauer et al. (1999, 2002) found significant amount (typically about 30–40% in particle mass) of alkanoic acid, alkanedioic acid and aromatic acid in the emission of vehicles in

Table 1
Chemical, gravimetric, SMPS mass concentrations (μg m^{-3}) and effective density (g cm^{-3}) of $PM_{0.1}$ at the tunnel (T), roadside (R) and forest (F).

	OM	EC	Ions	Elements	Total chem. conc.	Gravimetric conc.	SMPS conc.	Effective density[a]	Effective density[b]
R	0.86 ± 0.07	0.36 ± 0.17	0.55 ± 0.21	0.25 ± 0.07	2.02	2.21 ± 0.59	1.78 ± 0.33	1.40	1.45
T	10.4 ± 1.7	9.2 ± 1.8	1.0 ± 0.5	5.2 ± 0.9	25.8	33.2 ± 6.5	28.2 ± 5.8	1.25	1.29
F	0.20 ± 0.04	0.08 ± 0.02	0.08 ± 0.02	0.05 ± 0.01	0.40	0.65 ± 0.31	0.49 ± 0.14	1.15	1.22

[a] Obtained based on the method of Spencer et al. (2007).
[b] Determined by chemical compositions.

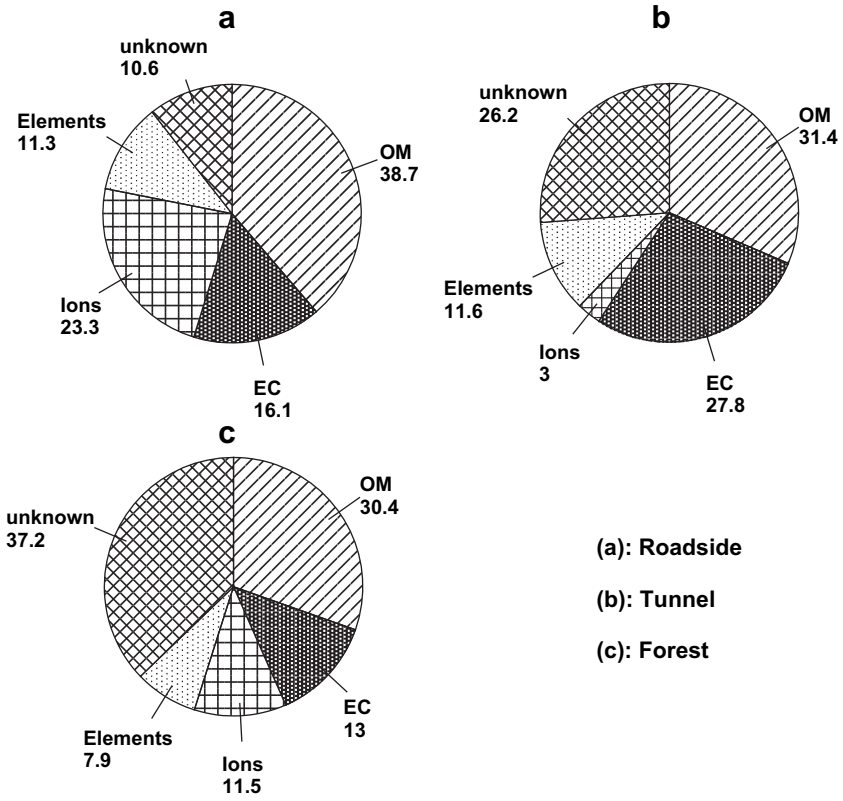

Fig. 5. Chemical compositions (%) of $PM_{0.1}$ (a) at Syuefu roadside, (b) in the Syueshan highway tunnel and (c) in the NTU Experimental Forest.

particulate phase, which are classified as water-soluble organics with high polarity. Thus, the tunnel particles would adsorb quite amount atmospheric moisture when the deliquescence RH was reached. In the present tunnel, a relatively low average RH of 42% (range: 35–50%) was observed compared with that in the forest and roadside. However, the average temperature was higher at 34 °C (range: 30–38 °C). Tang and Munkelwitz (1993) found that the deliquescence RH of the multi-component aerosols tends to decrease with an increasing temperature. In addition, the calculated absolute atmospheric water content in the tunnel was higher than that of the roadside based on Eqs. (1)–(3). Thus, it was expected that the conditions in the tunnel still reached the deliquescence point of aerosols. Therefore, the unexplained mass of 26.2% in the tunnel $PM_{0.1}$ was also attributed to aerosol water in this study.

Since the chemical compositions of $PM_{0.1}$ at the three sites were determined accurately and the unexplained $PM_{0.1}$ mass was assumed to be water in the present study, the effective density based on the chemical compositions could be calculated. In the calculation, the density of each chemical species of $PM_{0.1}$ was referred to that found in the literature. Turpin and Lim (2001) found the average density of OM in urban $PM_{2.5}$ was 1.2 g cm^{-3}, which was used as the density of the OM of $PM_{0.1}$ at the roadside and tunnel directly. Kavouras et al. (1999) used the density of 1.0 g cm^{-3} to convert the number concentration of forest OM of $PM_{0.003-0.2}$ to the mass concentration. This value was used for the OM of the forest $PM_{0.1}$ in this study. In addition, the present results showed SO_4^{2-} and NH_4^+ were the two most abundant ionic species at all three sites. The average density of 2.0 g cm^{-3} found by Sioutas et al. (1999) was used for these ions. In Park et al. (2003), the density of soot particles of 50 nm in mobility diameter was found to be 1.0 g cm^{-3} while the material density of EC was 2.0 g cm^{-3}. The EC in the $PM_{0.1}$ at all three sites had the particle diameter between 0 and 50 nm. Thus, the average density of EC in $PM_{0.1}$ was assumed to be 1.5 g cm^{-3}. The average density of elements in $PM_{0.1}$ should be smaller than the bulk density of their counterpart materials since the particle-bound elements were formed as oxides in aggregates. Therefore, the average effective density of the total elemental species was assumed to be 1.5 g cm^{-3}. Because the element mass was only about 10% of $PM_{0.1}$ mass at all three sites, the use of element density of 1.5 g cm^{-3} did not contribute very much to the effective particle density. Finally, the density of water, 1.0 g cm^{-3}, was used for the aerosol water mass. According to the above assumptions, the effective density of $PM_{0.1}$ at the roadside, tunnel and forest was calculated to be 1.45, 1.29 and 1.22 g cm^{-3}, respectively. Because the density of water (1.0 g cm^{-3}) is relative low compared with other chemical species of particles, particles with higher content of water, such as those in the forest, should have lower density. The data in this study supports this hypothesis and indeed the forest has the smallest average particle effective density than that at the tunnel and roadside.

The effective density of $PM_{0.1}$ calculated based on the chemical compositions and determined by using the method of Spencer et al. (2007) is shown in Table 1. It is seen that $PM_{0.1}$ effective density determined by using the chemical compositions is in good agreement with that calculated by the method of Spencer et al. (2007). The former is slightly higher than the later by less than 6%. Because of this agreement, it is foreseeable that the number concentration of the SMPS can be converted using the effective density determined by Spencer et al. (2007) for the real time measurement of the PM_{01} concentration without the prior knowledge of chemical compositions of $PM_{0.1}$.

4. Summary and conclusions

In this study, $PM_{0.1}$ at different atmospheres including a roadside, a highway tunnel and a forest was investigated. In addition to

the gravimetric analysis of $PM_{0.1}$, chemical compositions including OC, EC, water-soluble ions and trace elements were also obtained. Good chemical mass closure for $PM_{0.1}$ was obtained by taking into account the OC artifact, which was 89.8, 73.8 and 62.8% at the roadside, tunnel and forest, respectively. The OC artifact was found to be as high as 51.6 ± 10.7%, 20.0 ± 5.4% and 85.6 ± 18.4% of $PM_{0.1}$ mass at the roadside, tunnel and the forest, respectively. The severe OC artifact in $PM_{0.1}$ at the forest and roadside is due to a relative low $PM_{0.1}$ mass concentration and a long sampling period compared to the tunnel.

According to the mass closure results of this study, it is found the unexplained percentage of particle mass was higher at the forest (37.2%) than the tunnel (26.2%) and roadside (10.6%), which was assumed to be aerosol water in this study based on the findings of Pilinis et al. (1989) and Demou et al. (2003). This study concluded that the atmospheric UPs at the present roadside, tunnel and forest have significant water content of 11–37% particle mass even after conditioning at the RH of 40–45% before weighing. The higher aerosol water content for forest $PM_{0.1}$ than that at the roadside and tunnel was due to higher RH and absolute atmospheric water content in the present forest than the other two locations. The present effective density of $PM_{0.1}$ calculated from the chemical speciation results is in good agreement with that based on the method of Spencer et al. (2007). The effective density of the forest $PM_{0.1}$ (1.22 g cm^{-3}) is found to be lower than that in the tunnel (1.29 g cm^{-3}) and roadside (1.45 g cm^{-3}) due to the high water content in the aerosol mass in the forest. By using Eqs. (1)–(3), the effective density of atmospheric UPs can be predicted accurately without the prior knowledge of their chemical compositions. Therefore, it is foreseeable that the number concentration of the SMPS can be converted to the mass concentration based on the effectively density for the real time monitoring of the $PM_{0.1}$ mass in the ambient air.

Acknowledgement

The financial support of the Taiwan EPA (EPA-96-U1U1-02-104 and EPA-97-U1U1-02-106) is gratefully acknowledged.

References

Aggarwal, S.G., Kawamura, K., 2009. Determination of aerosol water content under near ambient humidity condition. Abstract in Asian Aerosol Conference, Bangkok, Thailand, Nov. 24–27, p. 15.

Chen, S.C., Tsai, C.J., Huang, C.Y., Chen, H.D., Chen, S.J., Lin, C.C., Chou, Charles C.-K., Lung, S.C., Roam, G.D., Wu, W.Y., Smolik, J., Dzumbova, L. Chemical mass closure and chemical characteristics of ambient $PM_{0.1}$, $PM_{2.5}$ and PM_{10} in a highway tunnel and at a roadside. Aerosol Science and Technology, submitted for publication.

Cass, G.R., Hughes, L.A., Bhave, P., Kleeman, M.J., Allen, J.O., Salmon, L.G., 2000. The chemical composition of atmospheric ultrafine particles. Philosophical Transactions of the Royal Society of London, Series A 358, 2581–2592.

De Carlo, S., Fiaux, H., A Marca-Martinet, C., 2004. Electron cryo-microscopy reveals mechanism of action of propranolol on artificial membranes. Journal of Liposome Research 14, 61–76.

Demou, E., Visram, H., Donaldson, D.J., Makar, P.A., 2003. Uptake of water by organic films: the dependence on the film oxidation state. Atmospheric Environment 37, 3529–3537.

Donaldson, K., Brown, D., Clouter, A., Duffin, R., MacNee, W., Renwick, L., Tran, L., Stone, V., 2002. The pulmonary toxicology of ultrafine particles. Journal of Aerosol Medicine—Deposition Clearance and Effects in the Lung 15, 213–220.

Ellison, G.B., Tuck, A.F., Vaida, V., 1999. Atmospheric processing of organic aerosols. Journal of Geophysical Research D 104, 11633–11642.

Fraser, M.P., Cass, G.R., Simoneit, B.R.T., 1998. Gas-phase and particle-phase organic compounds emitted from motor vehicle traffic in a Los Angeles roadway tunnel. Environmental Science and Technology 32, 2051–2060.

Geller, M.D., Sardar, S.B., Phuleria, H., Fine, P.M., Sioutas, C., 2005. Measurement of particle number and mass concentrations and size distributions in a tunnel environment. Environmental Science and Technology 39, 8653–8663.

Hänel, G., 1976. The properties of atmospheric aerosol particle as functions of the relative humidity at thermodynamic equilibrium with the surrounding moist air. Advances in Geophysics 19, 73–188.

Kavouras, I.G., Mihalopoulos, N., Stephanou, E.G., 1998. Formation of atmospheric particles from organic acids produced by forests. Nature 395, 683–685.

Kavouras, I.G., Mihalopoulos, N., Stephanou, E.G., 1999. Secondary organic aerosol formation vs primary organic aerosol emission: in situ evidence for the chemical coupling between monoterpene acidic photooxidation products and new particle formation over forests. Environmental Science and Technology 33, 1028–1037.

Kavouras, I.G., Stephanou, E.G., 2002. Direct evidence of atmospheric secondary organic aerosol formation in forest atmosphere through heteromolecular nucleation. Environmental Science and Technology 36, 5083–5091.

Kelly, W.P., McMurry, P.H., 1992. Measurement of particle density by inertial classification of differential mobility analyzer-generated monodisperse aerosols. Aerosol Science and Technology 17, 199–212.

Khlystov, A., Stanier, C., Pandis, S.N., 2004. An algorithm for combining electrical mobility and aerodynamic size distributions data when measuring ambient aerosol. Aerosol Science and Technology 38 (S1), 229–238.

Kleeman, M.J., Schauer, J.J., Cass, G.R., 2000. Size and composition distribution of fine particulate matter emitted from motor vehicles. Environmental Science and Technology 34, 1132–1142.

McMurry, P.H., Wang, X., Park, K., Ehara, K., 2002. The relationship between mass and mobility for atmospheric particles – a new technique for measuring particle density. Aerosol Science and Technology 36, 227–238.

McRae, G.J., 1980. A simple procedure for calculating atmospheric water vapor concentration. Journal of the Air Pollution Control Association 30, 394–396.

Nenes, A., Pilinis, C., Pandis, S.N., 1998. ISORROPIA: a new thermodynamic equilibrium model for multiphase multicomponent marine aerosols. Aquatic Geochemistry 4, 123–152.

Oberdörster, G., Oberdorster, E., Oberdorster, J., 2005. Nanotoxicology: an emerging discipline evolving from studies of ultrafine particles. Environmental Health Perspectives 113, 823–839.

Pak, S.S., Liu, B.Y.H., Rubow, K.L., 1992. Effect of coating thickness on particle bounce in inertial impactor. Aerosol Science and Technology 16, 141–150.

Park, K., Cao, F., Kittelson, D.B., Mcmurry, P.H., 2003. Relationship between particle mass and mobility for diesel exhaust particle. Environmental Science and Technology 37, 577–583.

Phuleria, H.C., Sheesley, R.J., Schaauer, J.J., Fine, P.M., Sioutas, C., 2007. Roadside measurements of size-segregated particulate organic compounds near gasoline and diesel-dominated freeways in Los Angeles, CA. Atmospheric Environment 41, 4653–4671.

Pilinis, C., Seinfeld, J.H., Grosjean, D., 1989. Water content of atmospheric aerosols. Atmospheric Environment 23, 1601–1606.

Schauer, J.J., Kleeman, M.J., Cass, G.R., Simoneit, B.R.T., 1999. Measurement of emissions from air pollution sources. 2. C_1 through C_{30} organic compounds from medium duty diesel trucks. Environmental Science and Technology 33, 1578–1587.

Schauer, J.J., Kleeman, M.J., Cass, G.R., Simoneit, B.R.T., 2002. Measurement of emissions from air pollution sources. 5. C-1–C-32 organic compounds from gasoline-powered motor vehicles. Environmental Science and Technology 36, 1169–1180.

Seinfeld, J.H., Pandis, S.N., 1998. Atmospheric Chemistry and Physics: from Air Pollution to Climate Change. John Wiley and Sons, New York, pp. 18–21, 507–519 and 1113–1192.

Shen, S., Jaques, P.A., Zhu, Y., Geller, M.D., Sioutas, C., 2002. Evaluation of the SMPS–APS system as a continuous monitor for measuring $PM_{2.5}$, PM_{10} and coarse ($PM_{2.5-10}$) concentration. Atmospheric Environment 36, 3939–3950.

Sioutas, C., Abt, E., Wolfson, J.M., Koutrakis, P., 1999. Evaluation of the measurement performance of the scanning mobility particle sizer and aerodynamic particle sizer. Aerosol Science and Technology 30, 84–92.

Spencer, M.T., Shields, L.G., Prather, K.A., 2007. Simultaneous measurements of the effective density and chemical composition of ambient aerosol particles. Environmental Science and Technology 41, 1303–1309.

Stein, S.W., Turpin, B.J., Cai, X.P., Huang, C.P.F., McMurry, P.H., 1994. Measurements of relative humidity-dependent bounce and density for atmospheric particles using the DMA-Impactor technique. Atmospheric Environment 28, 1739–1746.

Subramanian, R., Khlystov, A.Y., Cabada, J.C., Robinson, A.L., 2004. Positive and negative artifacts in particulate organic carbon measurements with denuded and undenuded sampler configurations. Aerosol Science and Technology S1, 27–48.

Tang, I.N., Munkelwitz, H.R., 1993. Composition and temperature dependence of the deliquescence properties of hygroscopic aerosols. Atmospheric Environment 27A, 467–473.

Tsai, I.Y., Kuo, S.C., 2005. $PM_{2.5}$ aerosol water content and chemical composition in a metropolitan and a coastal area in southern Taiwan. Atmospheric Environment 39, 4827–4839.

Turpin, B.J., Lim, H.-J., 2001. Species contributions to $PM_{2.5}$ mass concentrations: revisiting common assumptions for estimating organic mass. Aerosol Science and Technology 35, 602–610.

Turpin, B.J., Saxena, P., Andrews, E., 2000. Measuring and simulating particulate organics in the atmosphere: problems and prospects. Atmospheric Environment 34, 2983–3013.

Zhu, Y., Hinds, W.C., Kim, S.H., Shen, S., Sioutas, C., 2002. Study of ultrafine particles near a major highway with heavy-duty diesel traffic. Atmospheric Environment 36, 4323–4336.